A dual-mode rechargeable lithium–bromine/oxygen fuel cell

Citation: Bai, Peng; Viswanathan, Venkatasubramanian and Bazant, Martin Z. "A Dual-Mode Rechargeable Lithium–bromine/oxygen Fuel Cell." Journal of Materials Chemistry A 3, 27 (June 2015): 14165–14172 © 2015 The Royal Society of Chemistry

As Published: http://dx.doi.org/10.1039/c5ta03335g

Publisher: Royal Society of Chemistry

Persistent URL: http://hdl.handle.net/1721.1/110556

Version: Author's final manuscript: final author's manuscript post peer review, without publisher's formatting or copy editing

Journal of Materials Chemistry A RSCPublishing

ARTICLE

A dual-mode rechargeable lithium-bromine/oxygen fuel cell

Cite this: DOI: 10.1039/x0xx00000x

Peng Bai,[a] Venkatasubramanian Viswanathan[a,c] and Martin Z. Bazant[a,b]

Received 00th January 2012,
Accepted 00th January 2012

DOI: 10.1039/x0xx00000x

www.rsc.org/

In order to meet the versatile power requirements of the autonomous underwater vehicles (AUV), we propose a rechargeable lithium-bromine/seawater fuel cell with a protected lithium metal anode to provide high specific energy at either low-power mode with seawater (oxygen) or high-power mode with bromine catholytes. The proof-of-concept fuel cell with a flat catalyst-free graphite electrode can discharge at 3mW/cm^2 with seawater, and 9mW/cm^2 with dilute bromine catholytes. The fuel cell can also be recharged with LiBr catholytes efficiently to recover the lithium metal anode. Scanning electron microscopy images reveal that both the organic electrolye and the bromine electrolyte corrode the solid electrolyte plate quickly, leading to nanoporous pathways that can percolate through the plate, thus limiting the cell performance and lifetime. With improved solid electrolytes or membraneless flow designs, the dual-mode lithium-bromine/oxygen system could enable not only AUV but also land-based electric vehicles, by providing a critical high-power mode to high-energy-density (but otherwise low-power) lithium-air batteries.

Broader context: Autonomous underwater vehicles (AUV) have important potential applications in energy and environmental science, such as ocean monitoring for climate analysis, marine animal observation, undersea oil platform and pipeline inspection, and remote surveillance of submerged structures, bridges, ships, and harbours. Seawater-based fuel cells for AUV are attractive for long-time missions, but have low power, below the needs of communication and propulsion, while Li-ion batteries offer higher power for short times (<1 hour). This paper presents a rechargeable dual-mode lithium-oxygen/bromine fuel cell capable of running on seawater at low power with bromine injected on demand for higher power, analogous to nitrous oxide fuel injection in race cars with traditional internal combustion engines. Besides AUV, this dual-mode concept could also be an enabling technology for land-based electric vehicles, by providing high-power operation to lithium-air batteries, whose high energy densities are otherwise compromised by low power.

Introduction

Fossil fuels are the dominant energy resources enabling rapid economic development around the world, especially in transportation.[1] Increasing energy demand has encouraged not only the development of sustainable, renewable power sources for a better environment in the coming decades, but also the exploitation of deep-sea oil reservoirs all over the globe, including the Arctic Ocean.[2] As already witnessed in the Gulf of Mexico oil spill in 2010, accidents and equipment failures in undersea fossil fuel extraction and transport can adversely affect the life and health of marine animals, humans and whole ecosystems.[3, 4] Given that the extreme environment around the undersea facilities does not permit frequent or long-time human access, autonomous underwater vehicles (AUV) have become powerful tools for remote inspections, e.g. tracking the oil plume.[5] Besides petroleum engineering, AUVs also have many other important applications related to energy and the environment, such as hydrographic observation[6] and seabed mapping[7] for climate science and marine ecology, remote inspection of wrecks, bridge platforms, harbours and other undersea structures for safety and security.[8]

A critical challenge for the development of AUV for these and other more versatile tasks in the future is to find a suitable power system.[8, 9] A wide range of electrochemical technologies has been suggested as power sources for AUV, such as Al/H_2O_2, NiCd, NiMH, and Li-ion batteries, as well as more advanced concepts, such as a semi-fuel cell using oxygen dissolved in seawater as the oxidant, and magnesium or lithium as the fuel.[9, 10] While these power sources have managed to fulfil specific tasks, the need for new power sources for marine applications still exists, because traditional battery systems, such as NiCd, NiMH and Li-ion, suffer from low energy density, while the metal-O_2 semi-fuel cell and other seawater batteries[11, 12] suffer from limited power density.

Here, we adopt the novel design of a hybrid-electrolyte Li-air battery[13] and propose dual-mode operation by modifying or changing the catholytes, which allows (i) a low-power mode by

reducing oxygen dissolved in water to support enduring tasks, such as computer hibernation, lighting, video recording, etc.; and (ii) a high-power mode by reducing bromine catholytes to meet surge requirements, such as orientation adjustment, fast propelling, and acoustic signal communications. The bromine catholyte could be prepared via an online-mixing process, as demonstrated for an aluminium-based seawater battery,[14, 15] which injects hydrogen peroxide as the reaction booster to the seawater stream, or carrying a tank of optimal catholyte separately. Both modes of the proposed concept possess high specific energy, using relatively low-cost, commercially available materials.

The cell design for the two modes of operation is shown schematically in Fig 1, where the key component is the solid-electrolyte plate of lithium superionic conductor (LISICON). To avoid chemical reduction of Ti(IV) in LISICON,[16] a buffer layer must be placed between lithium metal and LISICON. One effective choice is lithium phosphorous oxynitride (LiPON).[17] West et al made a high-performance protected lithium metal anode by sputtering LiPON directly onto the LISICON plate, followed by thermally evaporating lithium onto the LiPON film to ensure intimate interfacial contact.[18] However, the low ionic conductivity of LiPON limits its thickness to less than a few microns,[19] which can result in the loss of intimate contact of the solid-solid interface during recharging cycles, and evaporating lithium metal requires a highly inert atmosphere. These practical and experimental issues can be avoided by using non-aqueous organic electrolyte as the buffer layer, thus forming a liquid-solid-liquid lithium-ion pathway between anode and cathode. This design was introduced by Zhang et al[13] in 2010 for a new type of lithium-air battery, but it was soon realized that flowing aqueous catholyte, instead of breathing air naturally, could achieve comparable performance even without using any catalyst.

Goodenough and Youngsik first investigated $Fe(NO_3)_3$ aqueous solution in a static liquid hybrid-electrolyte cell, but found that the cell has a short life since the catholyte attacks the Ti(IV) of the solid electrolyte.[20] Lu and Goodenough then demonstrated a flow cell using 0.1M $K_3Fe(CN)_6$ solution as the catholyte, a layer of carbon paper or porous nickel as the diffusion layer and current collector.[21] Through this pioneering work, Lu, Goodenough and Youngsik summarized the possible redox species for aqueous catholytes.[22] In the same year, Wang et al[23, 24] independently demonstrated the same concept in a static cell, using 0.1M $FeCl_3$ solution as the catholyte and a titanium mesh as the current collector. Zhao, Wang and Byon later extended the chart of redox couples suitable for aqueous cathodes[22] by adding the data of solubility, since it is the mathematical product of the redox potential and the solubility of the species determines the specific energy (Wh/kg) and energy density (Wh/L) of the aqueous cathode.[25] They then identified iodine as one promising candidate, and explored the possibility of I_2/I_3^- both in a static liquid cell[25-27] and a flow cell.[28] Along this line of research, Zhao et al. further investigated the feasibility of using dilute bromine catholyte in a static liquid cell.[29] Different from the design of the above systems, Chang et al. paired a coated lithium metal anode,[30] which has a hydrophobic polymeric layer between lithium metal and LISICON, with a tiny glassy carbon electrode in a more concentrated bromine catholyte to achieve much better performance.[31] More recently, Takemoto and Yamada[32] investigated the impedance of their static liquid cell, and correlated the increase of internal resistance to the chemical and structural degradation of LISICON. Their findings suggest that a Li^+-depletion layer will develop into the surface of the LISICON, even after three days of soaking in bromine catholytes.

While it may be easier to fabricate a static liquid battery, the closed design prevents the cell from working at the maximum power density, since the corresponding voltages are always well below the voltage of hydrogen evolution.[21, 22, 28, 29] The internal pressure built up in the cathode chamber due to gas generation will eventually rapture the fragile LISICON plate and instantly suffocate the cell. These issues can be managed, and the power enhanced, in a flow system.

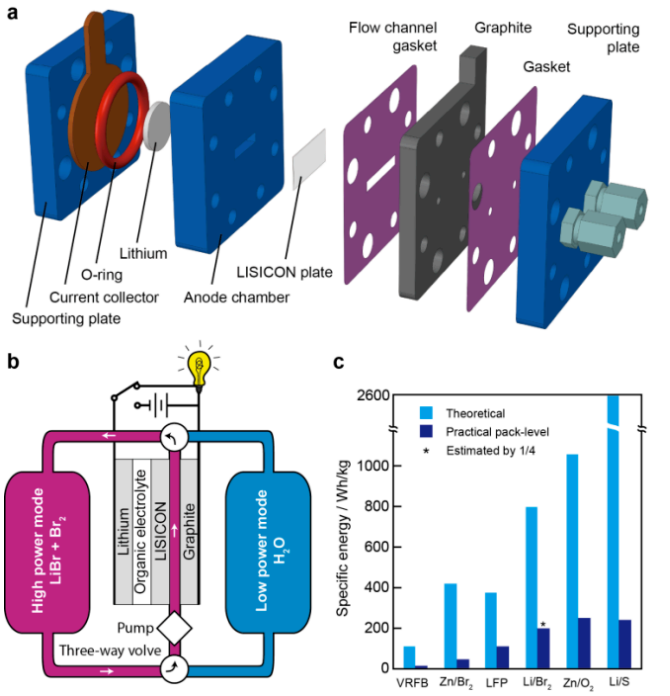

Figure 1. (a) Exploded view of the hybrid-electrolyte fuel cell. (b) Schematic demonstration of the dual-mode operation of the fuel cell. (c) Comparison of the theoretical and practical pack-level specific energies of lithium-bromine (Li/Br2) energy systems, all vanadium redox flow battery (VRFB), zinc-bromine flow battery (Zn/Br2), LiFePO4 (LFP), zinc-air battery (Zn/O2) and lithium-sulphur battery (Li/S). Data of Li/Br2 was calculated at the solubility limit, others were taken from reference[33].

In this study, we design and fabricate a rechargeable lithium-bromine/oxygen fuel cell using the liquid-solid-liquid design of the hybrid electrolyte system and a catalyst-free graphite plate as the cathode and current collector. We investigate the performance of the cell with various catholytes containing dissolved oxygen. We present polarization curves, demonstrate the feasibility of dual-mode operation at constant

voltages, and analyse the morphological changes of the aged LISICON plates.

Cell Design

Low power mode

Developing seawater batteries and fuel cells has a long history. However, the use of metal anodes remained elusive until the development of the LISICON protection layer.[10] This allows lithium metal to be paired with an aqueous electrolyte. The proposed design here uses oxidation of lithium metal at the anode according to the following equation,

$$Li \rightarrow Li^+ + e^- \quad (1)$$

which has the standard potential at −3.04V v.s. SHE, and possess a theoretical capacity of 3861mAh/g.

For the cathode, the first desired reaction during discharge is the reduction of the dissolved oxygen in seawater,

$$O_2 + 4e^- + 2H_2O \rightarrow 4OH^- \quad (2)$$

which has a standard potential that depends on the pH of the catholyte and is given as the relation U^o=1.23–0.059×pH. It must be noted that the solubility of oxygen in seawater is typically smaller than 1mM. The desired four electron reduction of oxygen typically requires a precious metal catalyst and suffers from large kinetic overpotentials. Hence, this mode can only generate moderate current densities and forms the low-power mode of the cell. The overall discharge product of reactions (1) and (2) is LiOH, which has a solubility of 5.3 M at 25°C.[34]

One of the important competing reactions at the cathode is the hydrogen evolution reaction, given by

$$2H_2O + 2e^- \rightarrow H_2 + 2OH^- \quad (3)$$

which also has a standard reduction potential that is pH dependent, according to the relation U^o=−0.059×pH. For the lithium-bromine static liquid battery, Zhao et al. suggested 3V as the safety limit to avoid H_2 evolution.[29] As they also set the upper limit of voltage to 4.35V to avoid oxygen evolution, pressure fluctuations in the cathode chamber of the static liquid cell could easily rapture the LISICON plate, after which lithium metal will quickly react with water chemically, and fail to supply electricity any more. Therefore, the cut-off voltages are rather the failure limits of the static liquid cell. This inevitable difficulty necessitates the open/flow system, which can better tolerate the pressure fluctuations and bring the gases out of the cathode chamber/channel along with the stream.

High power mode

To achieve a higher power output, an extra oxidant that can operate in a similar voltage range as the low power mode and compatible with an aqueous electrolyte is necessary. Bromine has been demonstrated in many flow battery systems,[35-37] and the reaction has very fast kinetics without the need for any precious metal based catalyst,

$$Br_2 + 2e^- \rightarrow 2Br^- \quad (4)$$

which has a standard potential of 1.09V v.s. SHE. The final discharge product in the high power mode is LiBr, which has extraordinary solubility of about 18.4 mol per kg of water at 25°C.[38, 39] The theoretical specific energy based on the solubility limit of LiBr is 791.5 Wh/kg, whose practical pack-level specific energy, estimated as ¼ of the theoretical value, could make ~200Wh/kg, superior to many existing systems,[33] e.g. $LiFePO_4$, as can be seen from Fig 1c.

pH of operation

The pH of catholytes is important. For the low power mode, changes of the pH will lead to the variation of the voltage. For the high power mode, while bromine reduction is the dominant reaction under acidic conditions, several other competing electrochemical processes are also possible under neutral and alkaline conditions.[29] More importantly, the stability of the LISICON plate is also pH dependent and has enhanced stability in neural to moderately basic environment.[40] Balancing these factors, we utilize a neutral pH environment for the catholyte striking compromise between kinetics of cathode reactions and the stability of the LISICON membrane. This design choice is also compatible with the pH of seawater, which is mildly alkaline with pH in the range of 7.5 to 8.4. At neutral pH, the OCV of the low power mode is 3.86 V and the OCV of the high power mode is 4.13 V.

In light of all the design considerations discussed above, we propose a scheme of dual-mode discharge, reducing either the species in seawater as the low-power mode, or the bromine and lithium bromide solution as the high-power mode. The system uses the high-power-mode catholyte for recharging. Proof-of-concept cells were fabricated and tested following the steps described in the Methods section.

Results

Electrochemical performance for various catholytes

As can be seen in Fig. 2a, the voltage of the cell varies linearly with respect to the current density, and the slope yields a conductivity in the same order of magnitude of the solid electrolyte, which is the main source of internal resistance and power limitation.

When deionized (DI) water is used as the catholyte, the cell works as a hybrid-electrolyte aqueous Li-air battery,[13] but exhibits large activation polarization since no catalyst is incorporated into the graphite cathode. The cell provides a peak power around 1.8 mW/cm^2 at 1V. When natural seawater collected from Boston harbour is used, the power density increases to 3 mW/cm^2 at a higher voltage around 1.5V, likely due to a higher concentration of dissolved oxygen.

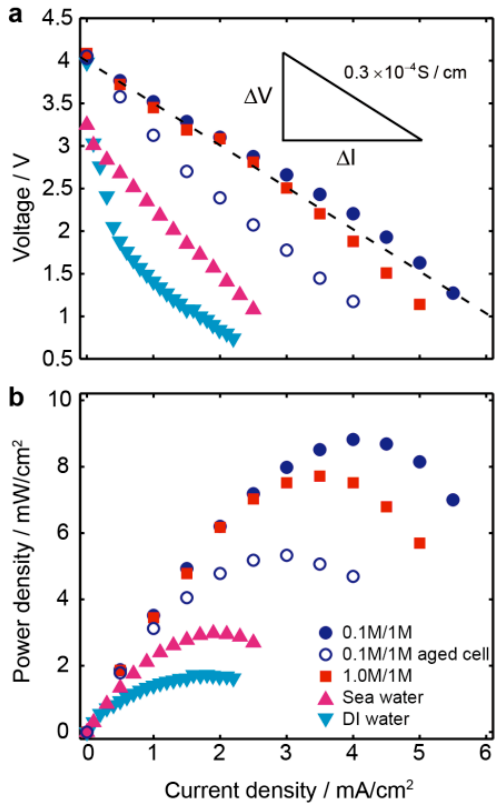

Figure 2 Discharging performance of the fuel cell with various catholytes at the flow rate of 1ml/(min·cm^2). (a) Voltage-current relation, and (b) the corresponding power density. 0.1M/1M stands for 0.1M Br2 in 1M LiBr solution.

In contrast, the performance is significantly improved with a dilute catholyte of Br_2 and LiBr solution, providing a peak power around 9 mW/cm^2 at 2.2V, which is consistent with the recent report of static Li-Br liquid battery.[29] The fact that increasing the concentration of Br_2 does not improve the discharge performance reveals that the rate-limiting process is not the transport in the catholyte, but the conduction of lithium ions through the solid electrolyte.[21] The deviation of high-concentration performance from the low-concentration performance at current densities larger than 3 mA/cm^2 is due to the degradation of LISICON. Such degradation becomes more significant after weeks of various experiments, and the slope of the polarization curve of the aged cell becomes much steeper that the fresh cell as shown in Fig. 2.

We tried to re-charge the cell with both DI water and seawater, neither of them can sustain a current as small as 0.025 mA/cm^2 at voltages up to 5V, which is to be expected given the lack of any added catalyst in the system. Figure 3 shows the polarization curves for charging processes with various bromine and lithium bromide catholytes. The conductivity estimated from the slope is consistent with that of discharge, again indicating the rate-limiting resistance of the LISICON layer. During recharging, increasing the concentration of Br_2 in the 1M LiBr solution results in clear increases of voltages, which can be viewed as a state-of-charge (SOC) dependent voltage behaviour that can be explained by Nernst equation. However for our open system, more importantly, we can manage to maintain a low concentration of Br_2 in LiBr catholyte, so as to ensure a current as high as possible for fast recovery of the lithium metal anode.

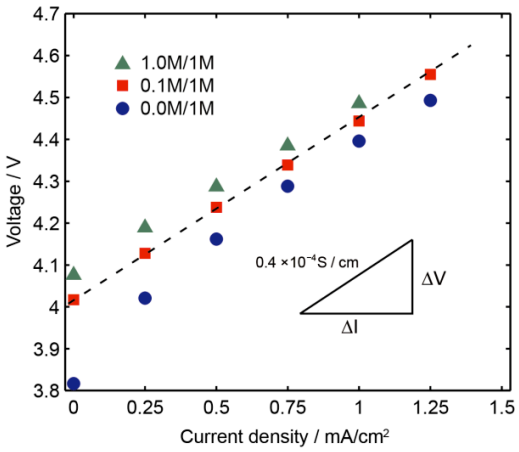

Figure 3. Charging performance of the fuel cell for three different catholytes at the flow rate of 1ml/(min·cm^2). 0.1M/1M stands for 0.1M Br2 in 1M LiBr solution, while 0.0M/1M means pure LiBr solution.

Dual-mode operation at constant voltages

The dichotomy in power output during dual-mode operation is best demonstrated by holding the cell at constant voltage and periodically switching the working catholytes. In order to reduce the mixing of two catholytes, a small segment of air is allowed into the tubing, and a higher flow rate, 3ml/(min·cm^2), is used. The experimental results are shown in Fig. 4. The values of the currents at 3V and 2V for different catholytes are consistent with those reported in Fig. 2, except that in Fig. 4b, the current of 0.1M/1M catholyte under 2V is much smaller, which is due to the degradation of LISICON as we shall see below. Note that cells used here had different corrosion histories, longer-time corrosion leads to higher resistance and thus lower current at the same voltage with the same electrolyte.

The polarization curve of one of our aged cells is included in Fig. 2 indicated by the open circles, which reveals the decaying conductivity of the system. Takemoto and Yamada suggested that the deterioration of the cell performance mainly comes from the degradation of LISICON, and more specifically the formation of a Li-ion depletion layer penetrating the surface of the LISICON. Here, to verify the source of degradation of the cell used in Fig. 4b, the cathode part of cell was first dissembled. Neither leakage of organic electrolyte, nor visible cracks were found on the LISICON plate, but some light brown stains can be seen in the region of the flow channel. The stains were carefully removed with wet paper tissues, and the surface of the LISICON plate was thoroughly washed with DI water. The graphite cathode was rigorously polished with sand paper for fresh surfaces and thoroughly washed with DI water as well. The re-assembled cell, however, did not recover the performance of a fresh cell, but became even worse. Opening the anode part afterwards, we found plenty of organic

electrolyte and a shiny lithium metal chip. These observations confirm that the degradation mainly comes from the LISICON plate, as Takemoto and Yamada also concluded, even though the LISICON plate is believed to be stable in seawater for up to two years.[41]

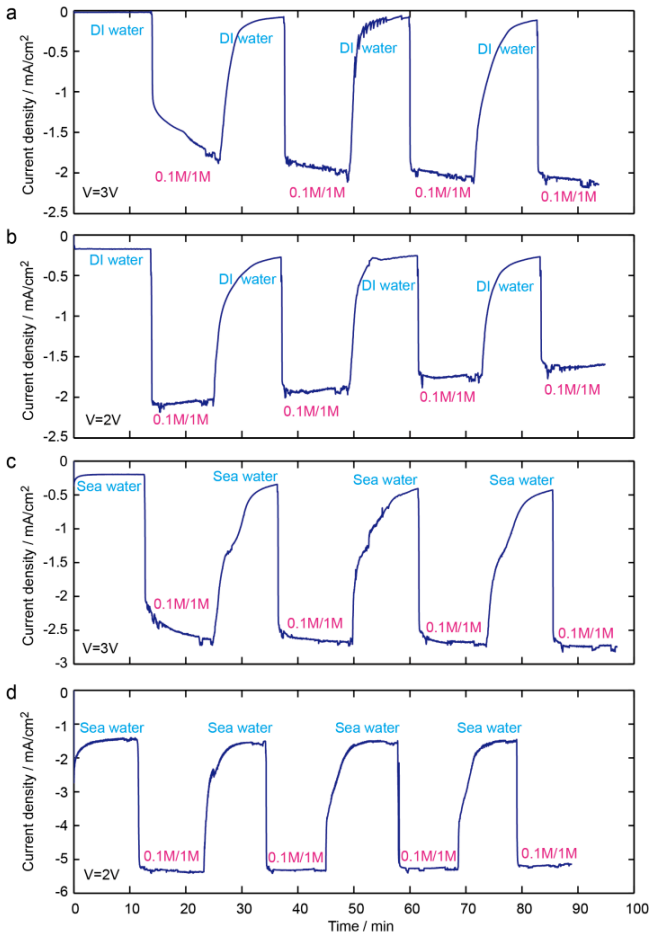

Figure 4. Dual-mode operations under constant voltages with DI water, sea water and high-power catholyte of 0.1M Br2 in 1M LiBr aqueous solution, at the flow rate of 3ml/(min cm^2). (a) DI water under 3V, (b) DI water under 2V, (c) Sea water under 3V and (d) Sea water under 2V.

Corrosion of LISICON plate

Figure 5 compares the morphological changes on the surfaces of the fresh and aged LISICON plates. The aged LISICON plate was in service for 2 weeks, contacting static organic electrolyte and flowing aqueous catholytes on either side. After being detached from the cell, the debris were collected into a small vial with DI water and applied sonication for 30 seconds, and then thoroughly washed with DI water without using sonication for four times. The samples were transferred to small petri dishes, dried at 50°C for 30 minutes, and kept in atmosphere before the scanning electron microscopy (SEM) observation. For the purpose of easier focusing, the new LISICON plate was lightly polished with a fine sand paper. While in a lower magnification, the surface of the plate looks smooth (Fig. 5a), very shallow cavities can still be seen in a higher magnification (Fig. 5b). In contrast, deep cavities can be easily identified on both surfaces of the aged LISICON plate. The surface in contact with aqueous bromine catholyte becomes very rough; flows of the catholytes flushed out shallow valleys on the surface (Fig. 5c). The surface in contact with static organic electrolyte looks perfectly flat, but surprisingly the density of the deep cavities is evidently higher than the other surface.

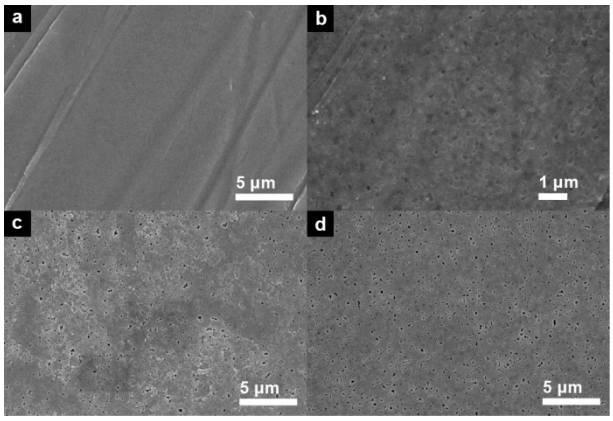

Figure 5. Scanning electron microscopy images of the surfaces of (a) new LISICON plate with scratches made by sand paper, (b) higher magnification of the new LISICON plate showing nano-sized shallow cavities, (c) Br2/LiBr catholyte-side of the aged LISICON plate, and (d) LiPF6/EC/DMC electrolyte-side of the aged LISICON plate.

Figure 6 provides SEM images of the cross sections of the same plates shown in Fig. 5. While the new plate looks dense and uniform throughout its whole thickness with very few nanopores, both surfaces of aged plate become rather porous, and nanopores can be observed everywhere in its cross section. These microscopic observations help explain the fact that it is very difficult to make scratches on the surface of the fresh LISICON plate with a single-edge blade, but much easier on the aged one.

Discussion

Analogous to the Nitrous Oxide System used in race cars, which injects N_2O to provide extra oxygen to increase the power output of the internal combustion engine, our dual-mode lithium-bromine/oxygen fuel cell allows the injection of bromine as the reaction booster to provide higher power density on demand. In practical applications to AUV, the low power mode with seawater can be used for computer hibernation, lighting, powering sensors and on-board equipment, while the high-power mode could significantly increase the propelling speed, or enable other high-power functions, such as acoustic signal transmission. In both cases, the high energy density provided by lithium metal allows extended working time undersea and opens up the possibilities of more versatile tasks.

This dual-mode design also holds promise for land-based electric vehicle applications. The catalyst-free high-power mode could be a good substitute of current Li-air batteries, which suffer from low power, low efficiency, low cycle life, and poor chemical stability,[16, 42, 43] while preserving a similar

high energy density. One way to realize this could involve circulating a small amount of water and mixing pure bromine into the stream to maintain the optimal concentration for desired power output. If designed in the lithium-abundant format, recharging the fuel cell requires simply refuelling the liquid bromine. In some extreme cases that bromine is no longer available on board nor nearby, the fuel cell can still provide electricity at a lower power, i.e. working as a modest lithium-air battery. When it is time to recover the lithium metal anode, highly concentrated LiBr solution can be used to enable fast electrochemical recharging of the fuel cell.

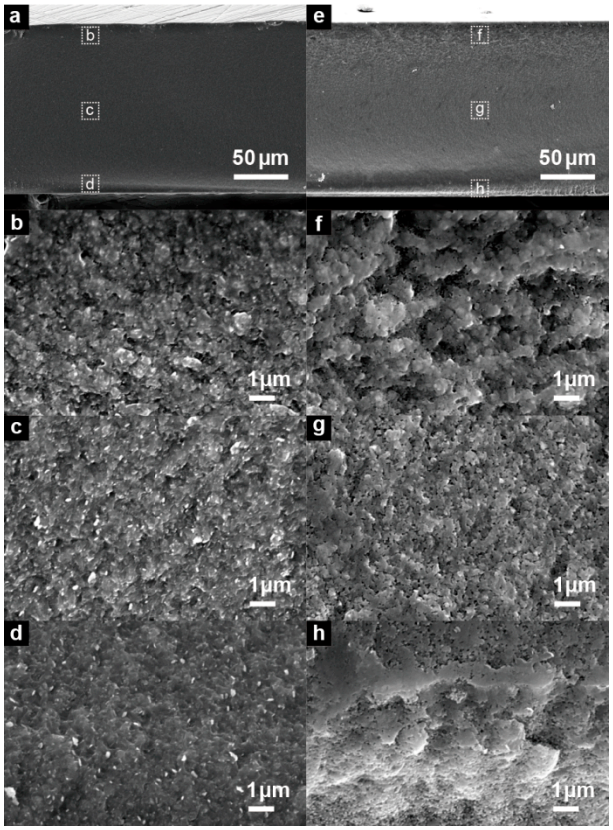

Figure 6. Scanning electron microscopy images of the cross-sections of (a-d) new and (e-h) aged LISICON plates. Compared with the images of the new plate, a 20-µm-thick porous layer was developed into the surfaces of the aged plate, and nanopores can be observed throughout the thickness.

The relatively low conductivity of the solid electrolyte plate limits the power output of the cell. However, as has been seen in the experiments, the estimated conductivities indicate extra Ohmic losses in the system. Besides reducing the thickness of both liquid layers, it is also important to optimize the cathode. Recent experiments have shown that the power density can be improved with a glassy carbon electrode[31] or a porous carbon electrode made of acetylene black and PVDF.[28, 29] Wang et al developed a carbon electrode by uniformly fixing 2-5nm LiBr particles on to the nanoporous structure of the conductive carbon black substrate.[44] While they only demonstrated the application of this novel electrode in a traditional lithium-ion battery, this electrode also holds promise for high power flow systems.

On the other hand, the chemical and mechanical robustness of the LISICON plate determines the life of the cell. While it is reported that the solid electrolyte remains stable in seawater for two years,[41] corrosion of the solid-electrolyte plate is not negligible.[32] For one of our oldest cells, organic electrolyte could come out through the mechanically intact LISICON plate when the internal pressure of the anode chamber is increased, either by tightening the anode chamber (compressing the silicone O-ring) or injecting more electrolyte. Water could percolate through the solid electrolyte and attack the lithium metal anode, well before the macroscopic disintegration of the solid electrolyte plate. The situation could be worse under the high pressure resulted from deep-sea environment. It is also worth noting that the 150-µm-thick LISICON plate is quite fragile, microcracks could be developed due to the imbalanced forces during assembling. Before a flexible water-stable solid electrolyte is developed, a hydrophobic polymer lining[31] between LISICON and lithium metal seems to be a viable approach to compensate the mechanical vulnerability of the LISICON plate and block water molecules coming through the cracks and porous networks.

Compared with cathode materials, water-stable solid electrolytes have received much less research attention. But as exemplified by this work and recent sodium-seawater fuel cells,[45, 46] solid-electrolyte-enabled rechargeable fuel cell could be a promising technology to harvest and utilize the clean "blue energy" in the ocean. Given that sodium is abundantly available in seawater, a dual-mode sodium-bromine/seawater fuel cell or flow battery could be an economical substitute to the proposed system. Developing better solid electrolytes is apparently the key to commercialize these technologies, but it may also become feasible to develop a membraneless system using immiscible electrolytes to replace the LISICON plate, which could increase the power output, extend the life of the cell and dramatically lower the cost of the system.

Conclusion

We have designed and fabricated a proof-of-concept rechargeable lithium-bromine/oxygen fuel cell that uses a solid-state LISICON plate to separate non-aqueous electrolyte and aqueous bromine catholyte. This design enables a dual-mode operation by changing the catholyte to deionized water or seawater, which could be applied to autonomous underwater vehicles for both long-time endurance operation and high-power activities. While the static liquid cell can only work between voltages of oxygen evolution and hydrogen evolution to avoid fractures of the LISICON plate due to the imbalance of the pressure, our flow system can better tolerate the gas evolution and thus can work in more extreme voltages to provide higher power density. We also show that organic electrolyte has a strong corrosive effect on the LISICON plate, which must be addressed before a long-lasting lithium-bromine rechargeable fuel cell can be developed, building on our proof of concept.

Methods

Cell fabrication

All components of the fuel cell were fabricated using traditional CNC machining or die cutting. As depicted in Fig. 1a, the cell was housed between two pieces of polyvinylidene fluoride (PVDF) porting plates. A piece of copper plate was used as the current collector, and a piece of lithium metal chip as anode. To accommodate the organic electrolyte between the lithium metal and the LISICON plate, a rectangular through hole was machined in a third PVDF plate, which also serves as the supporting plate to anchor four bolts for assembling components of either side of the LISICON plate. A small piece of LISICON plate was cut off by a diamond scriber, and bound to one side of the supporting PVDF plate by a thin layer of epoxy, and cured for at least 24 hours. The anode part was then assembled accordingly in an Ar-filled glove box, and sealed by a silicone O-ring between the copper current collector and the supporting PVDF plate. The organic electrolyte was injected into the anode chamber by a syringe as the last step. The cathode part was assembled in ambient environment. Flow channel of the catholyte was defined by a compressible Teflon gasket, whose thickness reduces to 300 μm after final assembly. A 6-mm-thick graphite plate was machined accordingly as the cathode, whose surface was simply polished with a sand paper. Another piece of gasket was placed between the graphite and the porting plate. The areas of the cross sections of the anode chamber and the flow channel are approximately the same 0.64 cm^2.

Materials

All chemicals were used as received. Bromine (ACS Reagent, >99.5%), lithium bromide (ACS Reagent, >99.5%) and the organic electrolyte (1 M LiPF6 in ethylene carbonate / dimethyl carbonate with a volume ratio of 1:1) were purchased from Sigma-Aldrich. The solid electrolyte plate (AG-01, Li_2O-Al_2O_3-SiO_2-P_2O_5-TiO_2-GeO_2, 10^{-4} S/cm, 25.4mm square by 150um) was purchased from Ohara Inc, Japan. Copper foil (3 mm thick, 99.5%), polyvinyliden fluoride (PVDF) plates, graphite plates, silicone o-rings and Teflon gasket tape (Gore) were all purchased from McMaster-Carr. PTFE tubing and fittings and peristaltic pumps were purchased from Cole-Parmer. Ultrapure deionized water was obtained from a water purification system (Model No. 50129872, Thermo Scientific). Seawater was collected in the Boston Old Harbour in Massachusetts and filtered with two layers of filter paper before experiments.

Electrochemical measurements

All electrochemical tests were conducted with an Arbin battery tester (BT-2043, Arbin Instruments) and cells were kept in a fume hood at room temperature. To obtain the polarization curve, a peristaltic pump and PTFE tubing were used to drive the catholyte flow at the rate of 1 ml/(min cm^2) until the open-circuit voltage reached a stable value. Then the cell was discharged or charged at certain currents for five minutes, whose response voltages usually stabilized in 1 minutes, but the reported values in this work are averaged voltages over the five minutes. The cell was flushed at 5 ml/(min cm^2) with DI water for 30 mins and air for 10 mins before introducing a different catholyte.

Acknowledgements

This work was supported by a seed grant from the MIT Energy Initiative.

Notes and references

[a] Department of Chemical Engineering, Massachusetts Institute of Technology, 77 Massachusetts Avenue, Cambridge, Massachusetts 02139, USA.

[b] Department of Mathematics, Massachusetts Institute of Technology, 77 Massachusetts Avenue, Cambridge, Massachusetts 02139, USA.

[c] Department of Mechanical Engineering, Carnegie Mellon University, 5000 Forbes Ave, Pittsburgh, Pennsylvanian 15217, USA.

1. M. Tran, D. Banister, J. D. K. Bishop and M. D. McCulloch, *Nat Clim Change*, 2012, **2**, 328-333.
2. A. Jernelov, *Nature*, 2010, **466**, 182-183.
3. B. D. Goldstein, H. J. Osofsky and M. Y. Lichtveld, *New England Journal of Medicine*, 2011, **364**, 1334-1348.
4. D. L. Valentine, J. D. Kessler, M. C. Redmond, S. D. Mendes, M. B. Heintz, C. Farwell, L. Hu, F. S. Kinnaman, S. Yvon-Lewis, M. Du, E. W. Chan, F. G. Tigreros and C. J. Villanueva, *Science*, 2010, **330**, 208-211.
5. R. Camilli, C. M. Reddy, D. R. Yoerger, B. A. S. Van Mooy, M. V. Jakuba, J. C. Kinsey, C. P. McIntyre, S. P. Sylva and J. V. Maloney, *Science*, 2010, **330**, 201-204.
6. C. C. Eriksen, T. J. Osse, R. D. Light, T. Wen, T. W. Lehman, P. L. Sabin, J. W. Ballard and A. M. Chiodi, *IEEE Journal of Oceanic Engineering*, 2001, **26**, 424-436.
7. Ø. Hasvold and N. Størkersen, *Journal of Power Sources*, 2001, **96**, 252-258.
8. S. Bhattacharyya and H. Asada, Control of a compact, tetherless ROV for in-contact inspection of complex underwater structures, 2014.
9. Ø. Hasvold, N. J. Størkersen, S. Forseth and T. Lian, *Journal of Power Sources*, 2006, **162**, 935-942.
10. S. J. Visco, E. Nimon, B. Katz, M.-Y. Chu and L. D. Jonghe, Lithium/air semi-fuel cells: high energy density batteries based on lithium metal electrodes, http://www.almaden.ibm.com/institute/2009/resources/2009/presentations/StevenVisco-AlmadenInstitute2009.pdf, 2015-04-29.
11. N. Shuster, Lithium-water power source for low power-long duration undersea applications, 1990.
12. N. Shuster, Google Patents, 1995.
13. T. Zhang, N. Imanishi, Y. Shimonishi, A. Hirano, Y. Takeda, O. Yamamoto and N. Sammes, *Chemical Communications*, 2010, **46**, 1661-1663.

14. R. P. Hamlen, B. Rao, W. Halliop and N. P. Fitzpatrick, Aluminum-hydrogen peroxide sea water battery, 1987.
15. B. M. L. Rao, S. Shah, J. Zakrzewski, R. Hamlen and W. Halliop, Multimode battery [marine system applications], 1990.
16. N. Imanishi and O. Yamamoto, *Mater Today*, 2014, **17**, 24-30.
17. X. H. Yu, J. B. Bates, G. E. Jellison and F. X. Hart, *J Electrochem Soc*, 1997, **144**, 524-532.
18. W. C. West, J. F. Whitacre and J. R. Lim, *Journal of Power Sources*, 2004, **126**, 134-138.
19. P. Knauth, *Solid State Ionics*, 2009, **180**, 911-916.
20. J. B. Goodenough and Y. Kim, *Chem Mater*, 2010, **22**, 587-603.
21. Y. H. Lu and J. B. Goodenough, *J Mater Chem*, 2011, **21**, 10113-10117.
22. Y. H. Lu, J. B. Goodenough and Y. Kim, *J Am Chem Soc*, 2011, **133**, 5756-5759.
23. Y. R. Wang, P. He and H. S. Zhou, *Adv Energy Mater*, 2012, **2**, 770-779.
24. Y. R. Wang, Y. G. Wang and H. S. Zhou, *Chemsuschem*, 2011, **4**, 1087-1090.
25. Y. Zhao, L. N. Wang and H. R. Byon, *Nat Commun*, 2013, **4**.
26. Y. Zhao, M. Hong, N. B. Mercier, G. H. Yu, H. C. Choi and H. R. Byon, *Nano Lett*, 2014, **14**, 1085-1092.
27. Y. Zhao, N. B. Mercier and H. R. Byon, *Chempluschem*, 2015, **80**, 344-348.
28. Y. Zhao and H. R. Byon, *Adv Energy Mater*, 2013, **3**, 1630-1635.
29. Y. Zhao, Y. Ding, J. Song, L. L. Peng, J. B. Goodenough and G. H. Yu, *Energ Environ Sci*, 2014, **7**, 1990-1995.
30. X. J. Wang, Y. Y. Hou, Y. S. Zhu, Y. P. Wu and R. Holze, *Sci Rep-Uk*, 2013, **3**.
31. Z. Chang, X. J. Wang, Y. Q. Yang, J. Gao, M. X. Li, L. L. Liu and Y. P. Wu, *J Mater Chem A*, 2014, **2**, 19444-19450.
32. K. Takemoto and H. Yamada, *Journal of Power Sources*, 2015, **281**, 334-340.
33. C. Wadia, P. Albertus and V. Srinivasan, *Journal of Power Sources*, 2011, **196**, 1593-1598.
34. P. Stevens, G. Toussaint, G. Caillon, P. Viaud, P. Vinatier, C. Cantau, O. Fichet, C. Sarrazin and M. Mallouki, *Ecs Transactions*, 2010, **28**, 1-12.
35. K. T. Cho, P. Ridgway, A. Z. Weber, S. Haussener, V. Battaglia and V. Srinivasan, *J Electrochem Soc*, 2013, **160**, X9-X9.
36. B. Huskinson, M. P. Marshak, C. Suh, S. Er, M. R. Gerhardt, C. J. Galvin, X. D. Chen, A. Aspuru-Guzik, R. G. Gordon and M. J. Aziz, *Nature*, 2014, **505**, 195-+.
37. W. A. Braff, M. Z. Bazant and C. R. Buie, *Nat Commun*, 2013, **4**.
38. M.-Y. Li, L.-S. Wang and J. r. Gmehling, *Industrial & Engineering Chemistry Research*, 2011, **50**, 3621-3631.
39. S. V. Stankus, R. A. Khairulin, V. A. Gruzdev and O. I. Verba, *High Temperature*, 2007, **45**, 429-431.
40. S. Hasegawa, N. Imanishi, T. Zhang, J. Xie, A. Hirano, Y. Takeda and O. Yamamoto, *Journal of Power Sources*, 2009, **189**, 371-377.
41. K. Nakajima, T. Katoh, Y. Inda and B. Hoffman, Lithium Ion Conductive Glass Ceramics: Lithium Ion Conductive Glass Ceramics, http://oharacorp.com/pdf/ohara-presentation-ornl-symposium-10-08-2010.pdf, 2015-04-08.
42. J. Lu, L. Li, J. B. Park, Y. K. Sun, F. Wu and K. Amine, *Chem Rev*, 2014, **114**, 5611-5640.
43. A. Manthiram and L. J. Li, *Adv Energy Mater*, 2015, **5**.
44. Y. L. Wang, X. Wang, L. Y. Tian, Y. Y. Sun and S. H. Ye, *J Mater Chem A*, 2015, **3**, 1879-1883.
45. J.-K. Kim, F. Mueller, H. Kim, D. Bresser, J.-S. Park, D.-H. Lim, G.-T. Kim, S. Passerini and Y. Kim, *NPG Asia Mater*, 2014, **6**, e144.
46. H. Kim, J.-S. Park, S. H. Sahgong, S. Park, J.-K. Kim and Y. Kim, *J Mater Chem A*, 2014, **2**, 19584-19588.

